

## Single-ion competing magnetic anisotropies in $\text{Pr}_x\text{Nd}_{1-x}\text{Co}_5$ intermetallic compounds

M. R. Ibarra, L. Morellon, and P. A. Algarabel

*Laboratorio de Magnetismo, Departamento de Física de Materia Condensada and Instituto de Ciencia de Materiales de Aragón (ICMA), Universidad de Zaragoza and Consejo Superior de Investigaciones Científicas, 50009 Zaragoza, Spain*

O. Moze

*Istituto di Struttura della Materia del Consiglio Nazionale delle Ricerche, Via E. Fermi 38, 00044 Frascati, Italy*  
(Received 21 June 1991)

Competing single-ion  $4f$  magnetic anisotropies have been studied within a noncollinear three-sublattice mean-field crystal-electric-field model in order to explain the observed complex magnetic behavior in the pseudobinary series  $\text{Pr}_x\text{Nd}_{1-x}\text{Co}_5$ . The interplay of different magnetic anisotropies gives rise to a contribution in the spontaneous free energy which turns out to have a minimum for the direction of the magnetization along a non-major-symmetry direction. A comparison with the experimental data of the spin-reorientation temperature and also with the thermal evolution of the spontaneous-spin-reorientation angle has allowed the determination of a reliable set of crystalline-electric-field parameters for the  $\text{Pr}^{3+}$  and  $\text{Nd}^{3+}$  ions. A calculation of the theoretical magnetization isotherms has been undertaken using these crystalline-electric-field parameters, in order to determine the theoretical magnetic anisotropy field, which has been compared for different temperatures and concentrations with experimental results obtained from singular-point-detection measurements.

### I. INTRODUCTION

During the past three decades a large amount of experimental work has been devoted to  $\text{RCo}_5$  ( $R$  = rare earth) intermetallics because of their use as starting materials for permanent-magnet applications. From this point of view, the characterization of their anisotropic behavior is of immense interest. These compounds crystallize in the hexagonal  $\text{CaCu}_5$  ( $P_6/mmm$ )-type structure. They are either ferromagnetic when  $R$  is a heavy rare earth or ferromagnetic in the case of the light ones, with a common feature, that is, a high Curie temperature ( $\approx 1000^\circ\text{C}$ ). Pioneering works concerning the crystallographic and magnetic behavior of these compounds<sup>1-3</sup> were the starting point for a quite extensive further characterization that, even up to this point, is still open and some of the magnetic features still remain not very well known. In the present paper we shall concentrate on the intrinsic magnetic properties of these compounds, studying the basic interactions that give rise to the highly anisotropic behavior. A great deal of previous investigations have been devoted to this topic.<sup>4-9</sup> There exist two different crystallographic sites for Co, while only one is available for the rare-earth ion.<sup>1</sup> The overall anisotropy of the Co sublattice can be inferred from the isomorphous compounds with a nonmagnetic rare-earth ion, e.g.,  $\text{YCo}_5$  and  $\text{LaCo}_5$ . It has been very well established that these compounds present axial anisotropy, with the easy magnetization direction along the  $c$  axis at all temperatures.<sup>10</sup> Nevertheless, the anisotropy of the rare-earth ion is imposed by the shape of the magnetic  $4f$  electronic shell in such a way that ions with a second-order Stevens' coefficient  $\alpha_J > 0$  (Er and Sm) present an axial anisotropy and, consequently, reinforce the Co sublattice anisotropy

while those  $R$  ions with  $\alpha_J < 0$  (Pr, Nd, Tb, Dy, Ho) tend to have an easy magnetization direction which lies in the basal plane of the hexagonal structure. In the last case we have the coexistence of two competing anisotropies, i.e., axial for the Co sublattice and planar for the  $R$  ion. As a general rule, at high temperatures the anisotropy of the  $3d$  band is predominant and will determine the overall anisotropy of the  $\text{RCo}_5$  compounds. However, at low temperatures, the interaction of the  $R$  ion with the crystalline electric field (CEF) and also the exchange interaction with the Co sublattice become very important and determine the overall anisotropic behavior of the system. This situation attains importance when both rare-earth and Co sublattice present a strong competition between their respective anisotropies. In such a case, spontaneous-spin-reorientation phase transitions can occur depending on their relative contributions to the free energy, with the final result being a noncollinear structure between Co and  $R$  magnetic sublattices in which the magnetic moments are oriented along non-major-symmetry directions.<sup>7,8</sup> Large applied magnetic fields can also induce first-order spin-reorientation transitions and these have been intensively studied in these compounds.<sup>11,12</sup> All of these peculiar types of behavior have as their origin a complex mixing of the rare-earth ion CEF and exchange energy levels. As a consequence of this, in order to give a detailed and physically realistic explanation of the anisotropic behavior in  $\text{RCo}_5$  compounds, we need to have a reliable set of CEF and molecular field parameters. However, the values found in the literature show a very large variance (see Table I). These have been determined by several different experimental techniques. Magnetic form factor and magnetization measurements have yielded some details about the com-

TABLE I. Crystal-electric-field and exchange parameters for  $\text{Nd}^{3+}$  and  $\text{Pr}^{3+}$  ions in pseudobinary  $\text{Pr}_x\text{Nd}_{1-x}\text{Co}_5$ . All the values are given in K.

Ion	$B_2^0$	$10^2 B_4^0$	$10^4 B_6^0$	$10^6 B_6^6$	$g_j \mu_B H_{\text{mol}}$	References
Pr	4.5				84	Greedan and Rao <sup>4</sup>
	-2.7	6.6			70	Ermolenko <sup>7</sup>
	2.4				40.3	Radwanski <sup>18</sup>
	$1.21 \pm 0.05$	$2.4 \pm 0.4$	$10.0 \pm 0.5$		$88 \pm 4$	This work
Nd	1.3				115	Greedan and Rao <sup>4</sup>
	3.1	-2.2		-1.46	98	Ermolenko <sup>7</sup>
	3.71	0.25	-5	-1.24	123	Lu <sup>17</sup>
	1.35				55	Radwanski <sup>18</sup>
	$3.0 \pm 0.1$	$0.16 \pm 0.02$			$121 \pm 6$	This work

bined effects of the CEF and exchange interaction.<sup>7,8</sup> From these measurements, an overall estimate can be gained about the relative strengths of the CEF and exchange interactions.

The aim of the present work is to give a detailed microscopic description of the anisotropic behavior and in the course of our recent research in the pseudobinary  $\text{Pr}_x\text{Nd}_{1-x}\text{Co}_5$  series.<sup>13,14</sup> The magnetic phase diagram can be delineated into three different regions through the series in the ordered phase (axis, cone, plane), as a direct consequence of spin-reorientation-transition (SRT) phenomena. For the two extreme concentrations,  $\text{NdCo}_5$  presents an axis-cone ( $T_{\text{SR}_1} = 280$  K) and cone-plane ( $T_{\text{SR}_2} = 241$  K) SRT with decreasing temperature, while  $\text{PrCo}_5$  presents a cone magnetic structure at temperatures below  $T_{\text{SR}} = 110$  K.

In the previous cited papers,<sup>13,14</sup> we reported in some detail the evolution of the cone angle with temperature and also with concentration as well as the magnetic anisotropy field. The basic idea of the present paper is to account for such experimental results by using a single-ion noncollinear CEF mean-field model. A noncollinear model is necessary because of the different anisotropies of the three ions, Pr, Nd, and Co. For example, in the easy-cone region it is expected that the R and Co sublattice moments are indeed no longer collinear since the R-Co exchange coupling is not strong enough to overcome the difference in the R sublattice anisotropy energy. Classical calculations<sup>15,16</sup> have clearly suggested that a noncollinear magnetic structure must occur during the spin-reorientation phase transition. In this framework, we have calculated the free energy of the system for different orientations of the easy magnetization direction for each magnetic sublattice, which turns out to be ferromagnetically exchange coupled. The minimum for such a free energy allows the effective easy magnetization direction for a determined temperature and concentration to be obtained. A comparison with the experimental results will give a set of CEF and exchange parameters for  $\text{Nd}^{3+}$  and  $\text{Pr}^{3+}$  in this series. The reliability of the determined parameters is intimately related to the capability of the model to explain the large amount of experimental results: magnetic phase diagram, thermal dependence of the SRT angle, and anisotropy field in all of the compounds of this series.

## II. BRIEF OUTLINE OF THEORY

In order to account for the anisotropic and magnetic behavior of mixed  $\text{Pr}_x\text{Nd}_{1-x}\text{Co}_5$  intermetallics, we shall consider a single-ion anisotropy for the rare-earth sublattice which has its origin in the electrostatic interaction of the magnetic  $4f$  electronic shell with the surrounding trivalent rare-earth ions. All the thermally excited energy levels in the ground  $J$  multiplet will be taken into account. Within this approximation we shall consider two contributions corresponding with the CEF energy of the  $\text{Pr}^{3+}$  ion ( $J=4$ ) and  $\text{Nd}^{3+}$  ( $J=\frac{9}{2}$ ), respectively. Of course, it is necessary to work in two different  $|LSJM_J\rangle$  subspaces in order to obtain the matrix elements of the CEF Hamiltonians, which, for this point symmetry ( $6/mmm$ ), is given by

$$\mathcal{H}_{\text{CEF}}^R = B_2^0 O_2^0 + B_4^0 O_4^0 + B_6^0 O_6^0 + B_6^6 O_6^6. \quad (1)$$

The splitting of the ground state for each ion ( $\text{Pr}^{3+}$ , ground state  $^3H_4$  and  $\text{Nd}^{3+}$ , ground state  $^4I_{9/2}$ ) can be obtained from the eigenvalues of the Hamiltonian in Eq. (1) and from these eigenvalues, the contribution of the anisotropy energy to the free energy,  $F_R$ , is obtained by calculating the partition function  $Z = \sum_i e^{-E_i/k_B T}$ , where  $E_i$  are the eigenvalues of Hamiltonian (1):

$$F_R = -x k_B T \ln Z^{\text{Pr}^{3+}} - (1-x) k_B T \ln Z^{\text{Nd}^{3+}}, \quad (2)$$

where  $T$  is the temperature and  $k_B$  the Boltzmann constant. This expression is necessarily based on the implicit assumption of a contribution proportional to each  $R^{3+}$ -ion concentration, which is again an indication of the single-ion origin for this interaction as well as a randomness of the ionic rare-earth substitution. Nevertheless, we are not interested in the pure CEF contribution to the anisotropy but in the physically realistic situation in which there exists a strong exchange coupling between the  $R^{3+}$  ionic and the Co magnetic moments, which, in turn, then split the pure CEF energy levels. This indirect (bilinear isotropic) interaction can be replaced by a single-ion effective Hamiltonian. This is the molecular field approximation, where the exchange interaction of a single-R ion with other ions is approximated by an effective molecular field  $\mathbf{H}_{\text{mol}}$ . The new energy level scheme will be calculated with addition of this important

exchange-interaction term in (1), which, in the molecular field approximation, can be written by

$$\mathcal{H}_{\text{ex}}^R = g_J \mu_B \mathbf{J}^R \cdot \mathbf{H}_{\text{mol}}^R. \quad (3)$$

The exchange contribution as discussed here is based on  $R$ -Co being coupled ferromagnetically. Although the  $R$ - $R$  exchange interaction is also present, because of the indirect origin of the exchange mechanism between both  $R$  sublattice, the relative value of this term with respect to  $R$ -Co is quite negligible. Then Co-Co exchange coupling is by far the largest contribution to the total energy, but, however, this term just introduces an isotropic reference level or a self-energy term, which need not be taken into consideration.

The interest lies in the calculation of  $F_R$  as a function of the angle that the magnetic moment makes with the  $c$  axis, which, in this case, is chosen as the quantization axis. Hence, the lowest value of  $F_R$  gives the easy magnetization direction. If we introduce  $\theta$  as the angle that the molecular field, which is along the Co magnetization direction, makes with the  $c$  axis, we can write the exchange Hamiltonian as

$$\mathcal{H}_{\text{ex}}^R = g_J \mu_B H_{\text{mol}}^R (J_z^R \cos \theta + J_x^R \sin \theta). \quad (4)$$

If we diagonalize the complete Hamiltonian  $\mathcal{H}^R = \mathcal{H}_{\text{CEF}}^R + \mathcal{H}_{\text{ex}}^R$ , the resulting set of eigenvalues and eigenvectors enables us to determine the effective anisotropic contribution given by expression (2), as well as the magnetic moment of each  $R$  sublattice,

$$\langle |\boldsymbol{\mu}^R| \rangle = g_J \mu_B \sqrt{\langle J_z^R \rangle^2 + \langle J_x^R \rangle^2}, \quad (5)$$

where the thermal averages  $\langle \rangle$  are calculated using the eigenvalues and eigenvectors  $|i\rangle = \sum a_{ij} |J, M_J\rangle$  of the Hamiltonian  $\mathcal{H}^R$ , in the form

$$\langle J_q^R \rangle = \frac{\sum_i \langle i | J_q^R | i \rangle e^{-E_i/k_B T}}{\sum_i e^{-E_i/k_B T}}. \quad (6)$$

In the calculation of total free energy  $F(\theta, T)$ , the axial cobalt sublattice anisotropy is represented by the phenomenological expression

$$E_k(T, \theta) = K_1(T) \sin^2 \theta, \quad (7)$$

where  $K_1$  is the anisotropy constant determined for  $\text{YCo}_5$ .<sup>17</sup> Consequently

$$F(T, \theta) = F_R(T, \theta) + E_k(T, \theta). \quad (8)$$

For each value of  $\theta$  we have calculated self-consistently the misalignment of the  $R^{3+}$  sublattice by using the thermal average of the projection of the magnetic moment on the quantization axis

$$\theta_R \equiv \tan^{-1}(\langle J_x^R \rangle / \langle J_z^R \rangle). \quad (9)$$

### III. RESULTS AND DISCUSSION

In following the former considerations, we have proceeded to account for the experimental results obtained in the above-mentioned previous works.<sup>13,14</sup> First, the

use of expression (8) has allowed us to calculate the thermal dependence of the angular evolution for the free energy of the system. In Figs. 1(a)–1(e) we represent the results obtained at selected temperatures for different concentrations. In all of them, we can see how, at a determined temperature, the minimum for that free energy starts to take place for a determined value of  $\theta$ , which constitutes an indication of the establishment of a spin-reorientation process. Taking as an example the results for  $x = 0.2$ , we can observe that, at 230 K, all of the magnetic sublattices lie along the  $c$  axis. However, at a lower temperature, for example,  $T = 220$  K, this minimum occurs for an intermediate direction giving rise to a conical noncollinear magnetic structure in which the cobalt sublattice makes an angle  $\theta$  ( $\theta = \theta_{\text{Co}}$ ) with the  $c$  axis. On the other hand, the  $\text{Nd}^{3+}$  and  $\text{Pr}^{3+}$  magnetic sublattices are oriented away from the  $c$  axis at angles  $\theta_{\text{Nd}}$  and  $\theta_{\text{Pr}}$ , respectively, in such a way that  $\theta < \theta_{\text{Pr}} < \theta_{\text{Nd}}$ . For lower temperatures, we have selected for this composition  $T = 110$  K, Fig. 1(a), in which the minimum on the free energy occurs at  $\theta = \pi/2$ , which means that, at this temperature and below, the compound is planar. Using the proposed model we can account for the magnetic behavior observed for the whole range of temperatures in this compound. A similar behavior has been predicted with this model for  $x = 0.4$  [see Fig. 1(b)]. Nevertheless, the results obtained in the case of high Pr concentrations show that, even at the lowest temperatures, the three magnetic sublattices remain oriented along intermediate non-major-symmetry directions, as can be observed in Figs. 1(c)–1(e). We have carried out this calculation for all compounds in this series and have succeeded in accounting for the magnetic phase diagram.

The CEF and exchange parameters determined and fitted in order to explain such behavior are reported in Table I where they are compared with previous results obtained by other authors.<sup>4,17,18</sup> In Fig. 2 we present the theoretical prediction for the critical lines which delimit the different regions in the magnetic phase diagram. These lines were obtained by determination of either the starting temperature, at which the effective easy magnetization direction deviates from the  $c$  axis, or the final one, at which it reaches the basal plane.

In a further step we have tested the reliability of the proposed model and also the determined CEF and exchange parameters. In this instance we have investigated the thermal evolution of the spontaneous-spin-reorientation angle  $\theta_{\text{eff}}$  with temperature. We consider  $\theta_{\text{eff}}$  as the angle that the effective magnetic moment  $\boldsymbol{\mu}_{\text{eff}}$  makes with the  $c$  axis, with  $\boldsymbol{\mu}_{\text{eff}}$  the vectorial sum of the different sublattice magnetic moments ( $\boldsymbol{\mu}_{\text{Co}}$ ,  $\boldsymbol{\mu}_{\text{Pr}}$ ,  $\boldsymbol{\mu}_{\text{Nd}}$ ). We illustrate in Fig. 3 a schematic situation underlying the basis of our calculation. Of course, such a noncollinear structure is established when the spin-reorientation-transition occurs. We present in Fig. 4 the results obtained using the CEF and exchange parameters summarized in Table I for Nd, Pr, and Co magnetic sublattice. As a result of this fitting, we can now that the results are indeed quite good. From these theoretical predictions, we can account quite accurately for the spin-reorientation temperature and also the thermal evolution

of the SRT angle. In a previous work,<sup>19</sup> in another different family of pseudoternary compounds of the type  $(\text{Er}_x\text{Dy}_{1-x})_2\text{Fe}_{14}\text{B}$ , we also found spin-reorientation phenomena taking place at low temperatures. A similar model also predicts a close behavior but, in this case, we considered a collinearity in the different magnetic sublattice.

The model has also been very valuable for the prediction of the thermal dependence of the intersublattice angles. We have no experimental evidence of these angles in this series and a microscopic experiment will be needed in order to test the obtained values. Nevertheless, evidence of such noncollinearity, has been observed in the isostructural compound  $\text{HoCo}_5$  (Refs. 8 and 9) by a com-

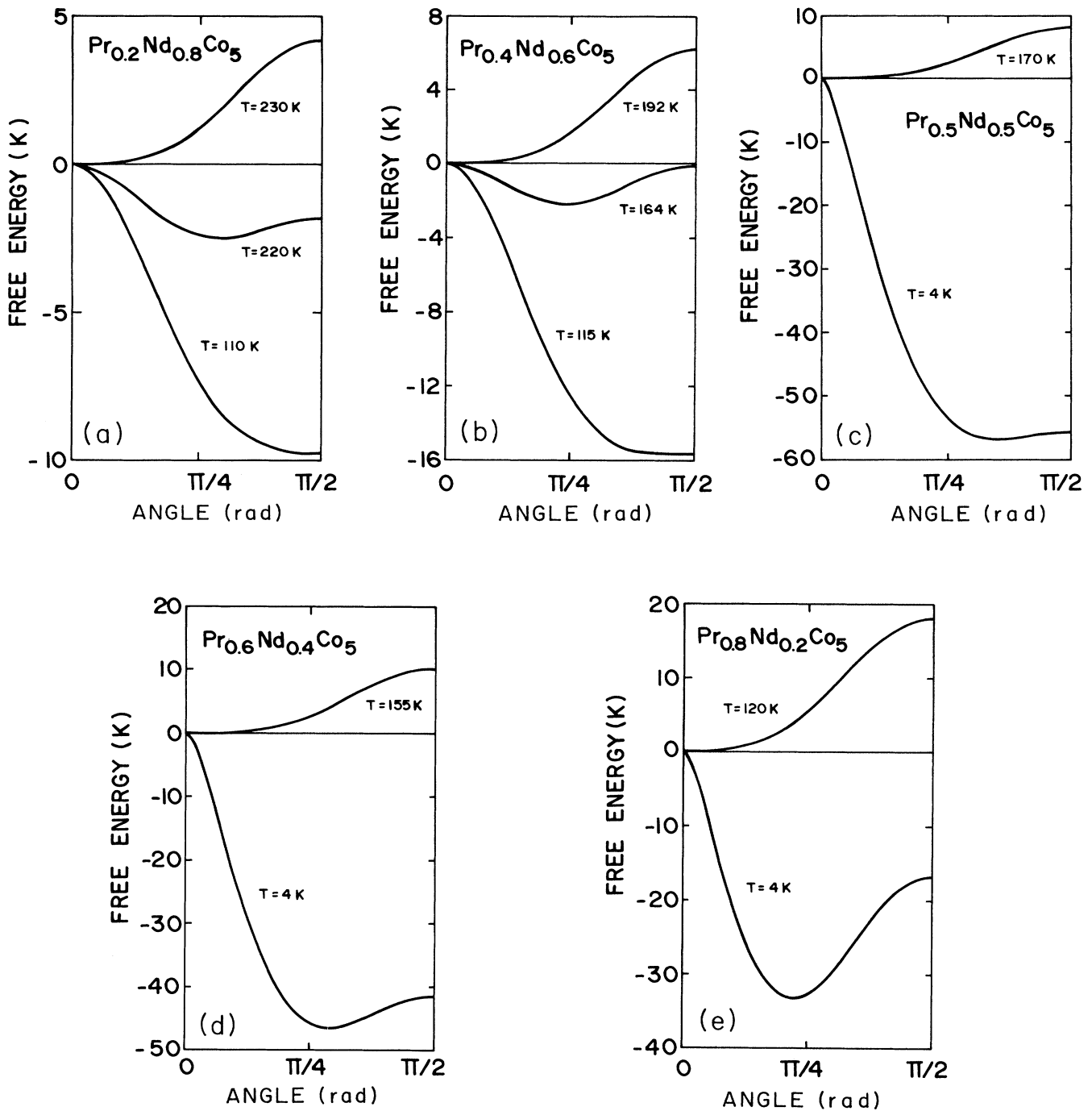


FIG. 1. Angular evolution of the free energy at several selected temperatures for compounds of the series  $\text{Pr}_x\text{Nd}_{1-x}\text{Co}_5$  using the parameters listed in Table I. (a)  $x = 0.2$ , (b)  $x = 0.4$ , (c)  $x = 0.5$ , (d)  $x = 0.6$ , and (e)  $x = 0.8$ .

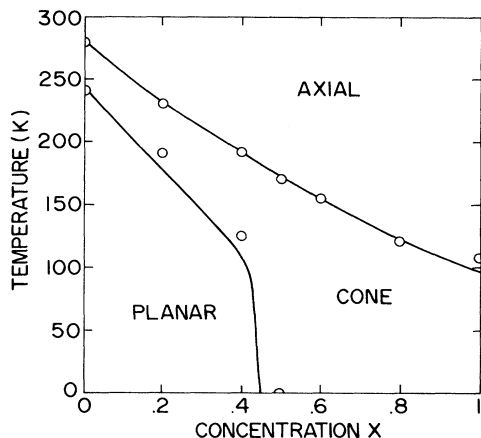


FIG. 2. Magnetic phase diagram of the series  $\text{Pr}_x\text{Nd}_{1-x}\text{Co}_5$ . (○) Experimental results (Ref. 13). The lines are theoretical model predictions.

bination of neutron-diffraction and Mössbauer spectroscopy on magnetically oriented samples. In Figs. 5(a) and 5(b) are displayed the model predictions for the intersublattice angles. At high-Nd concentration, we can observe a very small non-collinearity between the magnetic sublattice during the spin-reorientation processes. This is a direct consequence of the relevance of the intensity of the Nd-Co sublattice exchange coupling. The calculated angle  $\theta_{\text{Pr}}$  is always close to  $\theta_{\text{Co}}$  in this process, as is expected from the anisotropic behavior of the Pr sublattice which tends to establish a cone magnetic structure at low temperatures. In fact, it is also the reason why the opening angle between the Co, Nd, and Pr sublattices increase for rich-Pr concentrations.

Another important test of the model has been the prediction of the magnetic behavior under an applied mag-

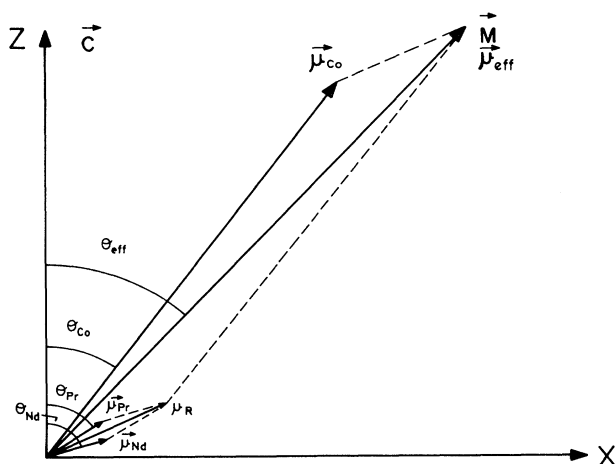


FIG. 3. Schematic representation of the different magnetic sublattice orientations in the spin-reorientation processes. The meaning of the different angles and vectors are explained in the text.

netic field ( $H_{\text{app}}$ ). In this case, an additional (Zeeman) term will appear in the Hamiltonian:

$$\mathcal{H}_z^R = g_J \mu_B \mathbf{J}^R \cdot \mathbf{H}_{\text{app}}. \quad (10)$$

Including this term in the total Hamiltonian  $\mathcal{H}^R = \mathcal{H}_{\text{CEF}}^R + \mathcal{H}_{\text{ex}}^R + \mathcal{H}_z^R$ , we have recalculated the free energy using expression (8) as a function of the angle of the different magnetic sublattice. We have obtained the equilibrium angle from the minimum in this free energy and calculated the magnetization for this equilibrium angle when the magnetic field is applied along either the  $c$  axis or in the basal plane.

In Figs. 6(a) and 6(c) we represent, at selected temperatures, the evolution of the calculated free-energy curves in  $\text{Pr}_{0.6}\text{Nd}_{0.4}\text{Co}_5$  for different values of the magnetic field, which is being applied in the basal plane. This kind of calculation has allowed us to determine the isotherm curves. As an example, in Fig. 7 we display the results obtained in the former  $x = 0.6$  compound. In this we represent the magnetization calculated along the applied magnetic field direction. Because, at 300 K, this compound has the  $c$  axis as the easy magnetization direction, the spontaneous magnetization will be zero in the basal plane, but as the magnetic field increases, the magnetiza-

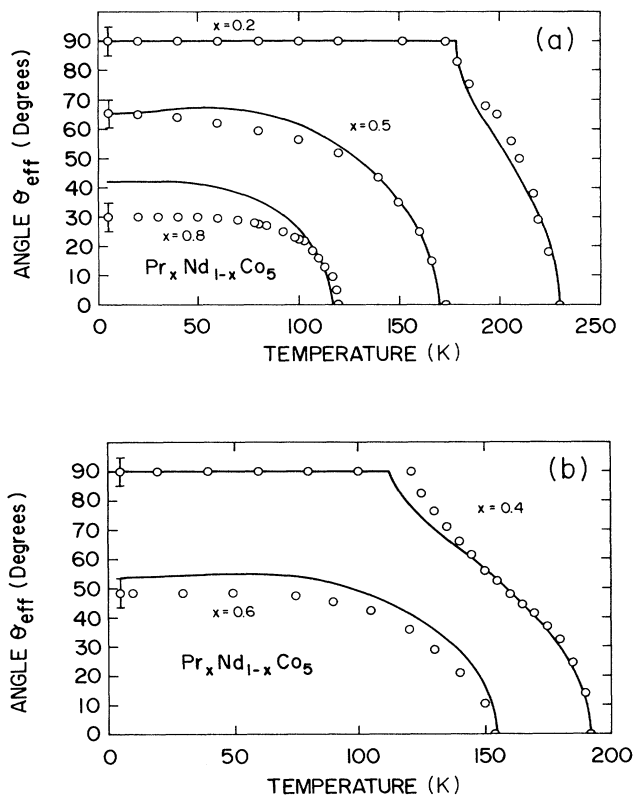


FIG. 4. Thermal dependence of the effective spin-reorientation angle  $\theta_{\text{eff}}$  for the pseudobinary series  $\text{Pr}_x\text{Nd}_{1-x}\text{Co}_5$ . (○) Experimental results, (—) theoretical predictions. (a)  $x = 0.2, 0.5, 0.8$ ; (b)  $0.4, 0.6$ .

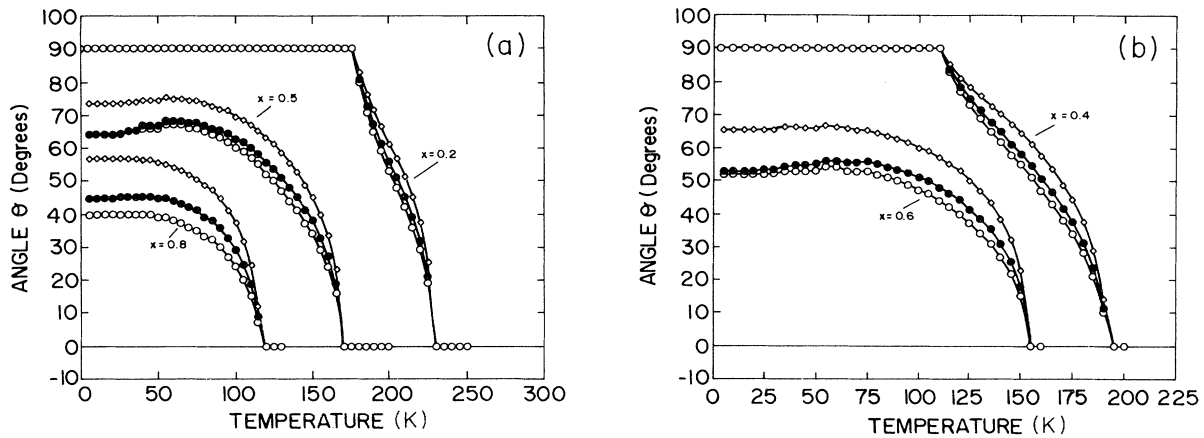


FIG. 5. Calculated thermal dependence of the spontaneous-spin-reorientation angle for the different magnetic sublattices using a noncollinear CEF mean-field model in  $\text{Pr}_x\text{Nd}_{1-x}\text{Co}_5$ , ( $\circ$ ) Co, ( $\bullet$ ) Pr, ( $\diamond$ ) Nd. (a)  $x = 0.2, 0.5, 0.8$ ; (b)  $x = 0.4, 0.6$ .

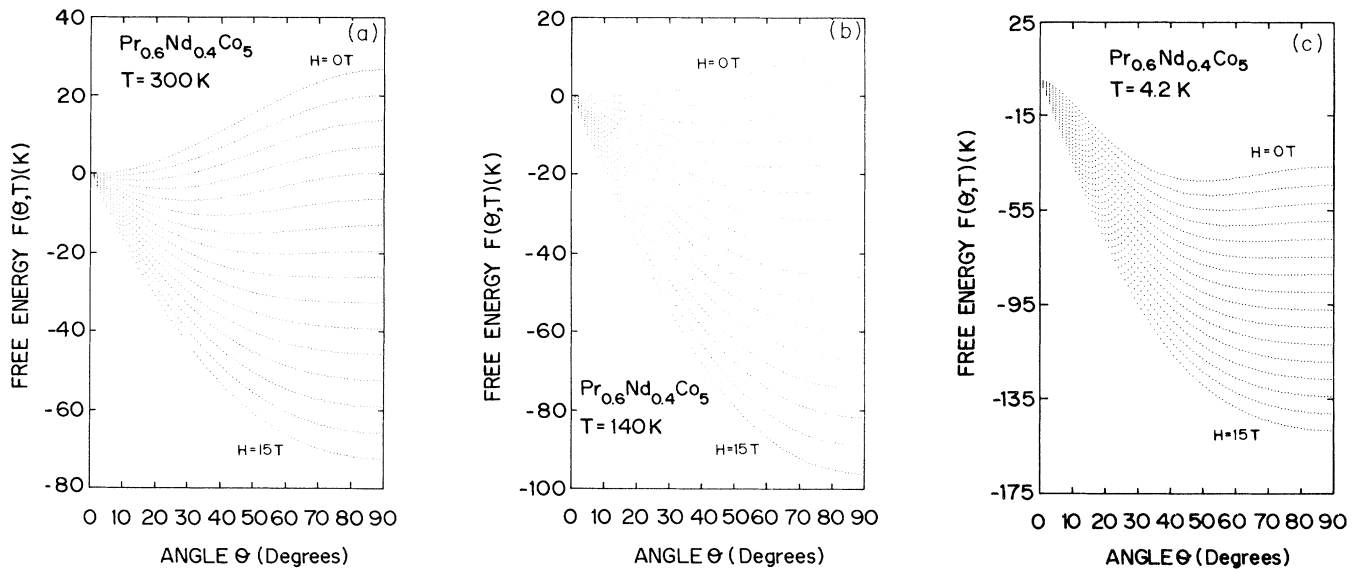


FIG. 6. Angular dependence of the calculated free energy at different values of the applied magnetic field, up to 15 T, in a step of 1 T for the compound  $\text{Pr}_{0.6}\text{Nd}_{0.4}\text{Co}_5$ . (a)  $T = 300$  K, (b)  $T = 140$  K, (c)  $T = 4.2$  K.

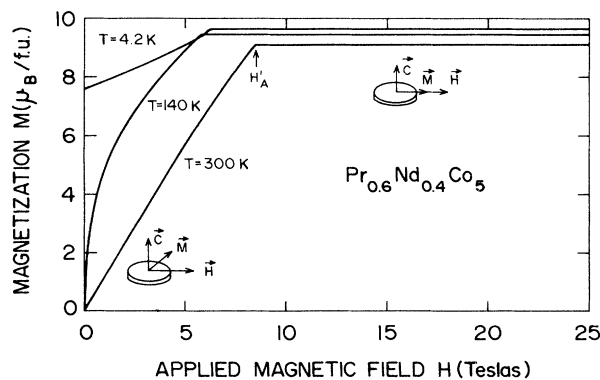


FIG. 7. Calculated isotherms of the magnetization along the direction of the applied magnetic field at the temperatures mentioned in Fig. 6 for  $\text{Pr}_{0.6}\text{Nd}_{0.4}\text{Co}_5$ .

tion rotates from the  $c$  axis to the plane, Fig. 6(a). The saturation will take place for the field value at which the applied magnetic field overcomes the torque that the anisotropy field makes on the magnetization in order to keep it along the easy magnetization direction. However, the situation is different at low temperatures, at 4 K the easy magnetization direction lies along an intermediate direction between the  $c$  axis and the plane. In this situation we have a spontaneous magnetization in the plane, Fig. 6(c), which increases with the applied magnetic field as a consequence of the rotation of the magnetization towards the field direction. The calculated isotherm curve

is represented in Fig. 7, in which we can also appreciate that the approach to saturation is different and can be related with the prediction for a first-order magnetization process (FOMP) anomaly type.

When we have SRT phenomena, it is useful to introduce two different anisotropy fields.<sup>19</sup> We shall consider  $H'_A$  the anisotropy field along the  $c$  axis and which will be associated with the saturation field in the plane, i.e., it is the anisotropy field that we measured when we apply the magnetic field along a direction in the plane.  $H''_A$  will be considered as the anisotropy field in the plane and is consequently related with the magnetic field that we need to

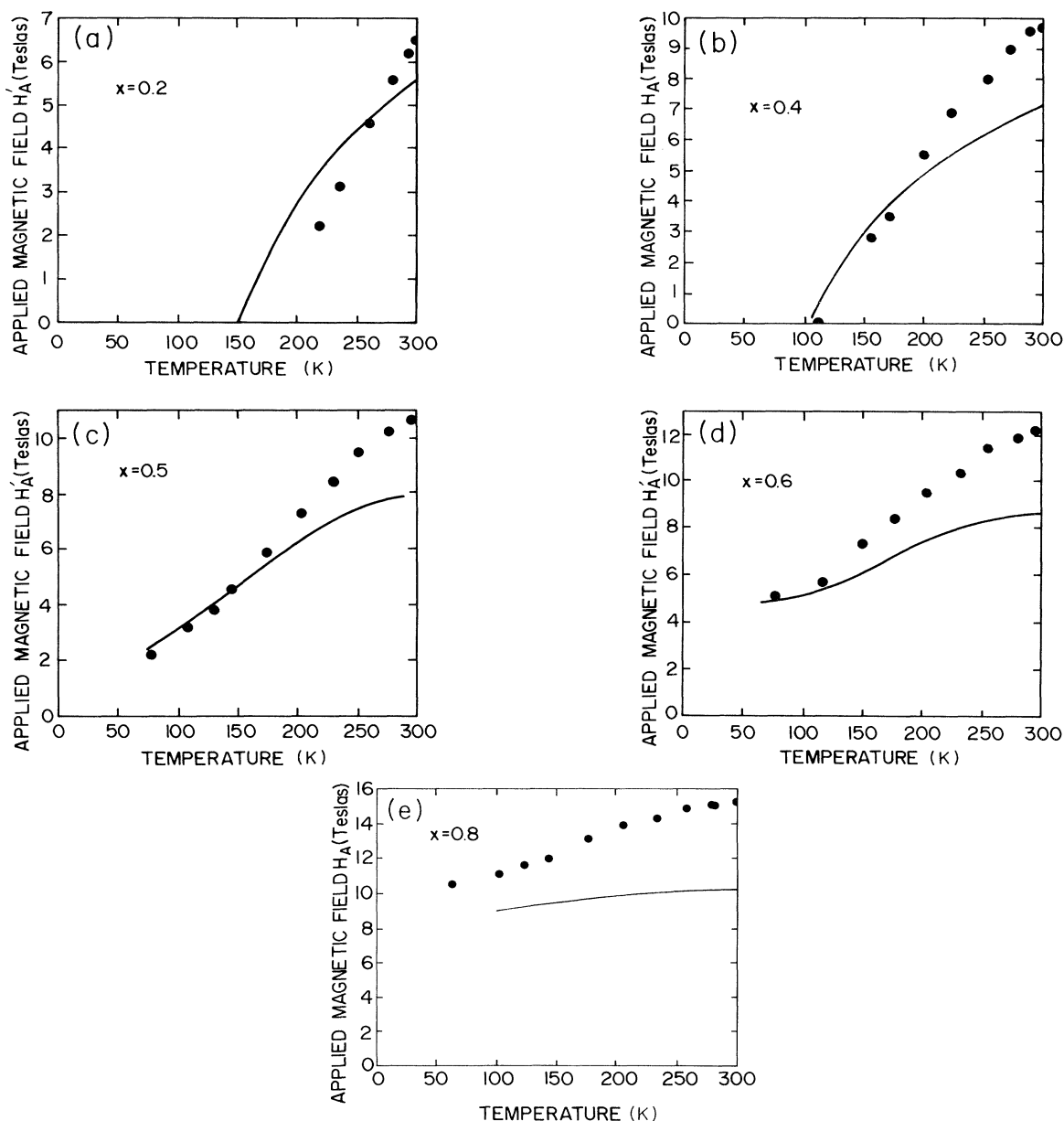


FIG. 8. Temperature dependence of the anisotropy field  $H'_A$  which is compared with the calculated saturation field along the basal plane for the compounds of the series  $\text{Pr}_x\text{Nd}_{1-x}\text{Co}_5$ . (●) are experimental results (Refs. 13 and 14), (---) theoretical predictions. (a)  $x = 0.2$ , (b)  $x = 0.4$ , (c)  $x = 0.5$ , (d)  $x = 0.6$ , and (e)  $x = 0.8$ .

apply along the  $c$  axis to saturate the sample, i.e., the anisotropy field that were measured in singular-point-detection (SPD) experiments when the magnetic field was applied along the  $c$  axis. As easily verified from their definitions, these anisotropy fields are related with the anisotropy constants  $K_i$  as

$$H'_A = (2K_1 + 4K_2 + 6K_3) / M_s, \quad (11a)$$

$$H''_A = 2K_1 / M_s. \quad (11b)$$

The aim of the present paper has also been to use the exposed microscopic three-sublattice model in order to explain the evolution of the anisotropy and critical fields obtained in the SPD experiment for different temperatures and concentrations. For such a purpose we have calculated a large number of isotherms for each concentration in order to give a theoretical prediction of the thermal evolution of  $H'_A$  and  $H''_A$ .

From our calculation it is very difficult to predict whether this saturation field corresponds either with an anisotropy field as result of a continuous approach to the saturation (second-order phase transition) or with a criti-

cal field at which the saturation is reached by a field-induced first-order phase transition. Such an extreme, however, was quite well established by SPD measurements. Nevertheless, we have found that the approach to saturation in the theoretical isothermal magnetization curves are different for those compounds which present a critical field, but, however, we have been unable to find any discontinuity similar to that due to a first-order phase transition in  $\text{PrCo}_5$ .<sup>17</sup> It should be remarked at this point that, in the  $R\text{Co}_5$  compound, such first-order transitions are, in general, barely perceptible. Single-crystal magnetization studies of  $\text{Nd}_x\text{Y}_{1-x}\text{Co}_5$  and  $\text{Pr}_x\text{Y}_{1-x}\text{Co}_5$  (Ref. 7) clearly demonstrate this. Simplified classical models forecast in both cases the existence of first transitions which were, in fact, not clearly experimentally observed. From this point of view, only a very slight hysteresis is observed in the experimental single-crystal magnetization curves, whereas calculations predicted a considerable hysteresis. In our case we have employed a more consistent quantum-mechanical description of the magnetization process.

In Fig. 8 we display the theoretical prediction for the

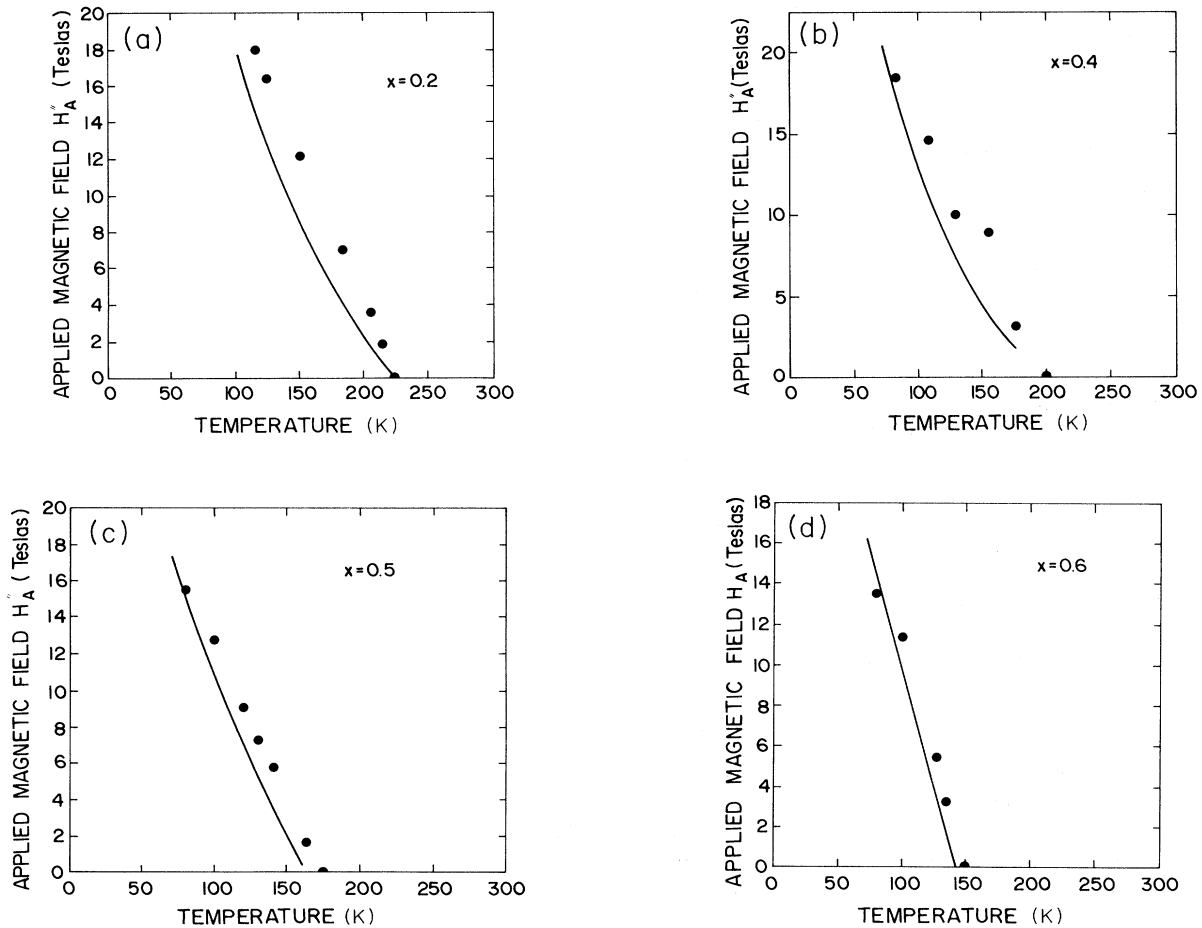


FIG. 9. Temperature dependence of the anisotropy field  $H'_A$ , which is compared with the calculated saturation field along the  $c$  axis for the compounds of the series  $\text{Pr}_x\text{Nd}_{1-x}\text{Co}_5$ . (●) are experimental results and (—) theoretical predictions. (a)  $x = 0.2$ , (b)  $x = 0.4$ , (c)  $x = 0.5$ , and (d)  $x = 0.6$ .



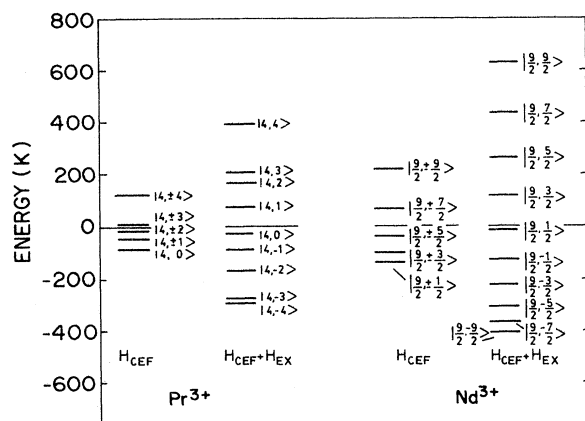


FIG. 10. Schematic diagram of the energy levels of the  $\text{Pr}^{3+}$  and  $\text{Nd}^{3+}$  ions in  $\text{Pr}_x\text{Nd}_{1-x}\text{Co}_5$  obtained using the parameters displayed in Table I. The molecular field is parallel to the  $c$  axis. The splitting of the pure CEF levels ( $H=0$ ) have been magnified twice for the sake of clarity.

anisotropy field  $H'_A$ , as a function of the temperature, obtained for different compounds of the series. A zero value for this field corresponds to temperatures at which the compounds present planar anisotropy. It is worth noting that the calculated values are in reasonably good agreement with the field, which experimentally is needed to rotate the magnetization towards the basal plane. This field has been determined in previous works<sup>13,14</sup> for temperatures below the spontaneous-spin-reorientation transition. For such a calculation, we have used the same set of CEF and exchange parameters, which are given in Table I for the whole of the compounds. This prediction, in our opinion, constitutes a very strict test of the reliability of the determined parameters.

The same kind of calculations have also been done in order to calculate  $H''_A$ ; in this case the magnetic field is applied along the  $c$  axis. High-Nd concentrations present low saturation fields at room temperature and tend to zero very quickly as we reach the temperature for the spontaneous-spin-reorientation transition. In Figs. 9(a)–9(e) we represent these results.

The large amount of experimental results recently obtained for the series  $\text{Pr}_x\text{Nd}_{1-x}\text{Co}_5$  has been the starting point of a systematic study of the magnetocrystalline anisotropy in  $R\text{Co}_5$  compounds. A microscopic model has been used to account for the anisotropy and exchange interaction. The noncollinear arrangement of the magnetic sublattice during the spin-reorientation process is implicit in the quantum-mechanical model used. This is because we have replaced the rare-earth ion magnetic moments by their quantum projection operators  $J_z$  and  $J_x$ , assuming the rotation in the  $z$ - $x$  plane where  $x$  is any direction in the basal plane. The self-consistent calculation of the magnetic moment can account for the thermal evolution of the spontaneous-spin-reorientation angle and satura-

tion field. We have explained, using the same set of parameters, in an overall quite satisfactory fashion, the magnetic phase diagram, the spontaneous-spin-reorientation angle, and the anisotropy fields.

To our knowledge, this is the first time that a quantum-mechanical description, with an implicit assumption of noncollinearity between a multisublattice, has been successfully used to account for anisotropic magnetic behavior in complex mixed  $R$  intermetallics.

Furthermore, we can equally say that the single-ion origin for the anisotropy in  $R\text{Co}_5$  has been exhaustively tested because the method followed has implicit this assumption in expression (2).

In general, the agreement between theory and experiment is quite good for rich-Nd concentrations, however, it is not quite satisfactory for high-Pr content. It is a normal observation that those parameters, which can explain relatively abrupt SRT, i.e., the axis-plane transition which takes place in a relatively large interval of the free energy  $[(F_p - F_A)/F]$ , are not necessarily as good when the final magnetic structure is conic. In such a case, the energy balance is quite delicate indeed and the excess energy with respect to the original easy-axis situation is rather small. In such a situation, other types of interactions, albeit small, most likely play an important role. Such interactions could have as their origin the dependence of the crystalline electric field on the distortion which arises at the spin reorientation and for lower temperatures due to the magnetoelastic coupling.<sup>20–22</sup> Another possibility could be the contribution from either the electric quadrupolar interaction or anisotropic exchange.<sup>23</sup> All of the aforementioned interactions constitute second-order perturbations that may indeed be significant in a situation where the interplay between different competing anisotropies nearly cancel out one another.

In a very recent publication,<sup>24</sup> additional results about CEF and exchange parameters have been offered considering a mixing of the  $J$  ground state with the first excited  $J'$  spin-orbit level. We have tested, in the course of our present investigation that the polarization of the wave function of the ground state by excited levels is practically negligible. In fact, the overall calculated splitting of the spin-orbit ground state for the  $\text{Pr}^{3+}$  and  $\text{Nd}^{3+}$  ions due to the CEF and exchange interactions is one order of magnitude less than the separation in energy between  $J$  and  $J'$  (see Fig. 10). Of course, if we impose in our calculation the condition of a considerable polarization of the ground-state wave functions by excited levels, we should choose quite unrealistic values for the CEF and exchange parameters.

#### ACKNOWLEDGMENTS

We are grateful to Professor A. del Moral for useful discussions and a critical reading of this paper. We also acknowledge the financial support of the Spanish CICYT through the Grant Nos. MAT88-68 and MAT90-1103. This work forms part of Project No. BREU-68-C supported by the European Communities.

- <sup>1</sup>J. H. Wernick and S. Geller, *Acta. Crystallogr.* **12**, 662 (1959).
- <sup>2</sup>H. Bartholin, H. B. Van Laor, R. Lemaire, and J. Schweizer, *J. Phys. Chem. Solids* **27**, 1287 (1966).
- <sup>3</sup>G. Hoffer and K. Strnat, *IEEE Trans. Mag. MAG-2*, 487 (1966).
- <sup>4</sup>J. E. Greedan and V. U. S. Rao, *J. Solid State Chem.* **6**, 387 (1973).
- <sup>5</sup>H. P. Klein, A. Menth, and R. S. Perkins, *Physica B* **80**, 153 (1975).
- <sup>6</sup>M. Okhoshi, H. Kobayashi, T. Katayama, M. Mirano, and T. Toushina, *Magnetism and Magnetic Materials-1975 (Philadelphia)*, Proceedings of the 21st Annual Conference on Magnetism and Magnetic Materials, AIP Conf. Proc. No. 29, edited by J. J. Becker, G. H. Lander, and J. J. Rhyne (AIP, New York, 1976), p. 616.
- <sup>7</sup>A. S. Ermolenko, in *Proceedings of the 3rd International Symposium on Magnetic Anisotropy and Coercitivity in RE-TM Alloys*, edited by J. Fidler (Technical University of Vienna, Vienna, 1982).
- <sup>8</sup>B. Decrop, J. Deportes, G. Givord, and R. Lemaire, *J. Appl. Phys.* **53**, 1953 (1982).
- <sup>9</sup>B. Decrop, J. Deportes, and R. Lemaire, *J. Less Common Met.* **94**, 199 (1983).
- <sup>10</sup>J. M. Alameda, D. Givord, R. Lemaire, and Q. Lu, *J. Appl. Phys.* **52**, 2079 (1981).
- <sup>11</sup>G. Asti, F. Bolzoni, F. Leccabue, R. Pannizzeri, L. Pareti, and S. Rinaldi, *J. Magn. Magn. Mater.* **15-18**, 561 (1980).
- <sup>12</sup>L. Pareti, O. Moze, M. Solzi, and F. Bolzoni, *J. Appl. Phys.* **63**, 172 (1988).
- <sup>13</sup>O. Moze, M. R. Ibarra, A. del Moral, G. Marusi, and P. A. Algarabel, *J. Phys. Condens. Matter* **2**, 6031 (1990).
- <sup>14</sup>O. Moze, G. Marusi, M. R. Ibarra, M. Solzi, and L. Pareti, *J. Magn. Magn. Mater.* **83**, 133 (1990).
- <sup>15</sup>S. Rinaldi and L. Pareti, *J. Appl. Phys.* **50**, 7719 (1979).
- <sup>16</sup>J. R. Cullen, *J. Appl. Phys.* **52**, 2038 (1981).
- <sup>17</sup>Q. Lu, Ph.D. thesis, Université Scientifique et Medicale de Grenoble, 1981.
- <sup>18</sup>R. J. Radwanski, *J. Magn. Magn. Mater.* **62**, 120 (1986).
- <sup>19</sup>M. R. Ibarra, P. A. Algarabel, C. Marquina, J. I. Arnaudas, A. del Moral, L. Pareti, O. Moze, G. Marusi, and M. Solzi, *Phys. Rev. B* **39**, 7081 (1989).
- <sup>20</sup>P. A. Algarabel, A. del Moral, M. R. Ibarra, J. B. Sousa, J. M. Moreira, and J. F. Montenegro, *J. Magn. Magn. Mater.* **68**, 177 (1987).
- <sup>21</sup>A. del Moral, P. A. Algarabel, and M. R. Ibarra, *J. Magn. Magn. Mater.* **69**, 285 (1987).
- <sup>22</sup>M. R. Ibarra, O. Moze, P. A. Algarabel, J. I. Arnaudas, J. S. Abell, and A. del Moral, *J. Phys. C* **21**, 2735 (1988).
- <sup>23</sup>R. Ballou, J. Deportes, and R. Lemaire, *J. Magn. Magn. Mater.* **70**, 306 (1987).
- <sup>24</sup>Zhao Tie-Song, Jin Han-Min, Guo Guang-hua, Han Xiu-feng, and Chen Hong, *Phys. Rev. B* **43**, 8593 (1991).